AIAA 96-3211

Fullerene Propellant Research for Electric Propulsion

John R. Anderson
Jet Propulsion Laboratory
Pasadena CA 91109

Dennis Fitzgerald
Jet Propulsion Laboratory
Pasadena CA 91109

32nd AIAA/ASME/SAE/ASEE
Joint Propulsion Conference and Exhibit
July 1-3, 1996 / Lake Buena Vista, FL

AIAA-96 3211

FULLERENE PROPELLANT RESEARCH FOR ELECTRIC PROPULSION

John R. Anderson* and Dennis litz.ge.raid*

Jet Propulsion Laboratory
California Institute of Technology
Pasadena, California

Abstract

The large mass, low first ionization potential and large electron impact ionization cross-section make Buckminsterfullerene (C_{60}) potentially attractive as an ion engine propellant. It has the potential for significant increases in engine, efficiency over that obtained with xenon at specific impulse.s less than 3,000 s. One problem encountered in fullerene ion engine.s has been dissociation of the propellant. Previously this was attributed to thermal decomposition rfuc to operation of the ion engine at temperatures greater than 1073 K. However, during tests conducted temperatures lower than 1073 K fullerene fragmentation was st ill observe.d. This prompted an investigation to determine if the dissociation was still duc to thermal effects or if it was duc to collisional processes in the discharge chamber. An ExB probe designed to discriminate between C_{60}^+ and C_{58}^+ was used to determine the composition of positively charged particles extracted from a filament cathode ion engine. Ideally only C_{60}^+ ions would be extracted from the ion engine; however, in addition to C_{60}^+ large quantities of fullerene fragment ions were observed. During these tests the ion engine. was operating at temperatures below 900 K and fullerene fragmentation was not detected in the vaporizer used to supply ions to the discharge chamber. However, after running the engine dissociated fullerene residue was found in the discharge Chamber. Typically this residue accounted for between 1/3 and 2/3 of the. C_{60} mass supplied to the discharge chamber during an experiment. From these. results it is evident that the fullerene dissociation is caused by processes inhere.nt to plasma production and not duc to thermal effects, provided the ion engine temperature is below 870 K. The amount of fragmentation observed during this testing seems to conflict with fragmentation cross- section data appearing in the literature. In the literature the appearance energy for fullerene fragment ions is greater than 45 eV; yet substantial fragmentation was ob.served when the ion engine was operated at lower discharge voltage.s. The apparent discrepancy can be resolve.(i by noting that electron impact ionization of C_{60} produces a metastable ion which has an energy dependent half-life before it fragments. In the cross- section experiments C_{60} is accelerated into the mass spectrometer within 1 to 10 µs of the time. at which it was ionized. In contrast the avc.rage reside.ncc time for a C_{60} in an ion engine. is two to three orders of magnitude longer (~1 ins). As a result more dissociation will be observed in an ion engine [Iron in the cross-section experiments even at lower electron energies. "1'here.fore, if fullerenes arc to be a useful propellant methods must be devised to efficiently process large amounts of C_{60} on much shorter time scales than those typical Of conventional ion engines.

Introduction

Because of the large mass, iow first ionization potential and large electron impact ioniz.alien cross-section, it has been suggested that use of Buckminsterfullerene (C_{60}) as a propellant might result in significant increases in ion engine efficiency over that obtained with xenon for missions requiring specific impulse in the 1,000 to 3,000 s range [1, 2]. Since 1991, three groups [3.5] have reported successful operation of arc discharge ion engines using fullerene as a propellant. Anderson and Fitzgerald [3] were able to extract beam currents between 2 and 3 mA from their device with a net accelerating voltage of 1.9 kV (corresponding to a C_{60} ion velocity of 22,500 m/s) and a minimum discharge voltage of 22 V. They con firmed the presence of fullerene ions by mass

* Member of Technical Staff, Advanced Propulsion Group, Member AIAA

spectral analysis of the extracted ion beam. Hruby et al. [4] detected fullerene material deposited on optical surfaces using Fourier transform infrared (FTIR) spectroscopy. Both of these groups reported substantial erosion of the filament cathodes used in their devices that ultimately resulted in cathode failure. In both of these sources, notable degradation of the propellant molecules at high temperature was confirmed by FTIR spectroscopic analysis of the powder remaining in the effusive cell and on the walls of the discharge chamber. Nakayama and Takegahara [5] extracted up to 33 mA beam currents with a net accelerating voltage of 0.7 kV. They report that a residue was found on the discharge chamber walls after operation of the thruster on fullerenes; however, they do not state whether the residue was composed of fullerenes or fullerene fragments.

Horak and Gibson [6] operated a commercially available Kaufman ion source with fullerenes for ion assisted deposition applications. They were able to sustain a discharge for 30 minutes while extracting a 50-100 $\mu A/cm^2$ beam of fullerene ions. They reported that approximately 10% of the initial mass of C_{60} was recovered from the discharge chamber as a mixture of graphitic carbon and fullerene. Fang et. al. [7] operated a hollow cathode ion source on a mixture of argon and fullerenes. The hollow cathode was operated on argon and fullerenes were introduced into the discharge chamber by argon carrier gas. They report detection of up to 1 nA of C_{60}^+ as well as fragment ions using a 90° analyzing magnet mass spectrometer.

The observed degradation of fullerenes in these reports is a concern because, over a long period of operation, the carbon residue could build up and plug hollow cathodes and propellant feed lines. Flakes of residue could also short out the optics system grids [8]. In addition, decreased thruster efficiency due to extraction of an ion beam with a distribution of charge-to mass ratio would result from extraction of ionized fullerene fragments. To determine if it is possible to eliminate fullerene fragmentation, the mechanism causing the degradation must be identified. Possible mechanism include, electron impact induced fragmentation, collisions with discharge chamber walls, photon induced fragmentation and thermal decomposition.

Since fullerenes became available in macroscopic quantities in 1990 [9], there have been several experimental studies of the electron impact fragmentation of C_{60} [10-12]. It is known that the main mechanism for fragmentation of C_{60}^+ is sequential loss of C_2. The first reaction in this chain is

$$C_{60}^+ -> C_{58}^+ + C_2 \quad . \qquad \text{(Eq. 1)}$$

Subsequent reactions are

$$C_{2n}^+ -> C_{2n-2}^+ + C_2 \qquad \text{(Eq. 2)}$$

for n= 29, 28,...,16. Below n= 16 the molecule does not form a fullerene closed-cage structure [13]. In these electron impact fragmentation experiments the fragment ion C_{58}^+ does not appear until the electron energy exceeds 45 eV. Typically ion engines are operated at discharge voltages below 45 eV; therefore, it was thought that electron impact induced dissociation was unlikely to account for the degradation observed in the ion engines.

There have been several studies of fullerene dissociation by accelerating ion into the surface of various materials [14, 15]. In these studies fullerenes had to be accelerated to over 200 eV kinetic energies before significant C_{58}^+ production was observed. In an ion engine ions can impact surfaces with kinetic energies as high as the discharge voltage. Again these energies are lower than those observed in the surface impact dissociation experiments it was considered unlikely that this could account for the observed degradation.

Experiments of photon induced dissociation [13, 16] showed that up to 20 eV photons were required before fullerene fragments were observed. The maximum temperature surface in the ion engines is the cathode filament which operates at temperatures on the order of 2000 K. At this temperature there are virtually no 20 eV photons produced, resulting in negligible fragmentation in the ion engine.

There have been several studies of the thermal stability of C_{60} [17-19]. Frum et al. [20] observed thermal degradation of C_{60} heated to 1223 K while studying its infrared emission spectrum, while Sundar et al. [19] observed that solid C_{60} decomposes into amorphous carbon upon heat treatment beyond 993 K for 24 hours. Leifer et al. investigated solid state fullerene decomposition kinetics [21]. Fullerene degradation is attributed to solid-state unimolecular decay with an activation energy of 266 kJ/mol over the temperature range from 1073 to 1173 K. In our previous work [3] with arc discharge ion engines the temperature had been greater than 1070 K so we attributed the observed fullerene decomposition to thermal degradation. In order to avoid significant propellant fragmentation, thruster operating temperatures must be maintained below approximately 1073 K.

This upper bound on temperature affects the maximum vapor pressure which can be achieved in the mass feed system. Several studies of fullerene vapor pressure as a function of temperature appear in the literature [22-25]. At 1073 K the vapor pressure of C_{60}

is approximately 130 Pa (1 Torr). To maintain a pressure on the order of 0.1 Pa (mid 10^{-4} Torr range), typically found in operating ion engine discharge chambers, requires a temperature of about 800 K. Therefore, the temperature window in which a fullerene thruster can be operated is between 800 and 1073 K.

To avoid the presence of high temperature hollow cathodes which typically operate at temperatures in excess of 1300 K, RF ion engines have been investigated. Takegahara and Nakayama [26] have reported an unsuccessful attempt to establish an RF-generated plasma using fullerenes. They found that their quartz discharge chamber wall temperature was too low, resulting in condensation of the fullerene propellant. Anderson et al. [27] also report an unsuccessful attempt to establish a RF discharge using fullerenes. They found that RF xenon discharges quench when small quantities of fullerene are introduced. Fullerenes have a large electron attachment cross-section and quenching is attributed to fullerenes scavenging free electrons from the plasma.

Further concern about fullerene degradation arose during the RF experiments because evidence of fragmentation was still observed even though the ion engine was at temperatures below 1073 K. This result would indicate that the observed fragmentation was not solely due to thermal effects but that electron impact and surface impact might cause more dissociation than expected based on the appearance energy for fragments. In their work, Fang et. al. [7] do not state the operating temperature of their ion source but they note that C_{60} dissociates at high temperatures. They also note that there is a discrepancy between their results and appearance energy data in the literature.

This paper describes work done to determine if the observed fullerene fragmentation was due to thermal degradation or due to processes occurring during plasma production.

Fullerene Ion Engine

To investigate fullerene decomposition during plasma production an arc-discharge ion engine with a filament cathode was constructed. It is recognized that fullerene impinging on the filament will dissociate; however, the probability that a fullerene will impact on the filament before being extracted through the optics system can be kept to a low value. This probability is approximately equal to the filament surface area to optics system open area. For the thruster described here this ratio is less than 2%. A schematic diagram and two photograph of the thruster are shown in Figs. 1-3.

The thruster, shown in Fig. 1, has a two-grid optics system and is mounted inside a 0.9 m diameter by 2.9 m long vacuum chamber capable of maintaining a no load pressure in the 10^{-4} Pa (10^{-6} Torr) range. The ion optics system consists of molybdenum screen and accelerator grids. They are spaced 1.3 mm apart and have 331 matching 2.4 mm diameter holes with center-to-center spacing of 3.0 mm for an open area fraction of 0.58. The accelerator grid bias supply (up to 100 mA D.C., 0.5 to 2.0 kV) is used to bias the accelerator grid negative with respect to ground. The screen grid, held at cathode potential, is biased positive with respect to ground by the screen grid bias supply (up to 100 mA D.C., 0.5 to 2.0 kV). With the exception of the accelerator grid the entire ion engine is biased positive with respect to ground by the screen grid bias supply.

The discharge chamber is enclosed at the downstream end by the optics system and along the diameter by a 70 mm diameter, 28 mm long molybdenum anode. The discharge chamber anode is wrapped with two heater wires to provide temperature control. Each 44 Ω heater wire has a variable power supply (up to 2 A A.C., 0 to 120V). The upstream end of the discharge chamber is a molybdenum baffle plate. The baffle plate is the interface between the discharge chamber and the oven which is used to vaporize fullerenes. The anode is electrically isolated from the screen grid and baffle plate by boron-nitride rings.

The filament cathode is heated to thermionic emission temperatures using the cathode heater supply (up to 6 A A.C., 0 to 15 V). Power leads to the cathode located at the center of the discharge chamber are through a twin bore ceramic tube (3.2 mm O. D., 0.9 mm bore diameter) which is inserted into the discharge chamber through a hole in the anode.

To determine if fullerene dissociation is due to thermal or plasma processes, it is desirable insure that plasma production does not occur in the same region as fullerene vaporization takes place. To decouple the discharge from the fullerene vaporization process the baffle plate has 169 holes with a length-to-diameter ratio of 4. The holes are 1.5 mm diameter and the plate is 6 mm thick. The oven and baffle plate are held at cathode potential to keep plasma from leaking through the baffle into the oven. The oven is a 70 mm diameter by 30 mm long molybdenum cup which is capped on the upstream end by the baffle plate. The oven diameter is wrapped with heater wire and the upstream end is equipped with a coil heater wire. The 64 Ω oven diameter heater wire and the 57 Ω oven coil heater wire each have a variable power supply (up to 2 A A.C., 0 to 120V).

To allow operation of the ion engine on various gases, a hollow ceramic tube (3.2 mm O.D., 1.6 mm I.D.) protrudes into the oven. Gases used to calibrate diagnostic equipment can be supplied through this tube.

To reduce the likelihood of fullerene spillage during ion engine assembly, fullerenes are placed in a quartz thimble before they are placed in the oven. When the oven is heated the fullerenes sublimate and effuse through the baffle plate into the discharge chamber. A small fraction of the fullerene mass flow is directed reward a water cooled Inficon mode.f XTM/2 quartz crystal micro-balance (QCM). Real-tin)c measurements of the rate at which fullerenes condense on the QCM can be correlated to the actual mass flow of fullerenes into the discharge chamber through a calibration constant.

The QCM used to monitor the fullerene flow rate is water cooled and the temperature of the Q('M holder was held below 300 K during all experiments which is cold enough 10 keep fullerenes from sublimating from the QCM. Because the geometry of the experimental apparatus does not change during a particular experiment, it is assumed that the fraction of the flow impinging cm the QCM remains constant as [he. flow rate and ion engine temperature vary. The system is taken apart between runs to resupply fullerenes to the own resulting in slight variations of alignment between the oven and QCM from run to run; therefore, calibration constants arc obtained for each run.

The calibration constant for total flow rate is determined by weighing the fullerene- filled quartz thimble bc.fore and after each run [0 find the total mass of evaporated material. This quantity is then divided by the. total accumulated mass on [he. QCM crystal to obtain the calibration constant C where

$$C = \frac{\Delta M}{\int_T \dot{m}_{qcm}\, dt} \qquad \text{(Eq. 3)}$$

and AM is the total mass sublimated from the crucible, $\dot{m}_{qcm}$ is the. mass flow condensing on the QCM and the integration is over the time T (luring which fullerenes flow to the, QCM. The actual mass flow rate. to the discharge chamber $\dot{m}$ i s

$$\dot{m} = (C- 1)\, \dot{m}_{qcm} \qquad \text{(Eq. 4)}$$

The QCM is located approximately 70 mm from the crucible. and fullerenes arc. directed toward the Q('M through a 1.4 mm diameter aperture in the oven. With this configuration, C typically varies between 6×10^3 and 8×10^3

Ion engine. temperatures arc monitored by thermocouples attached 10 the outer diameter at the upstream and downstream end of both the anode and oven.

A photograph of the assembled ion engine is shown in Fig. 2. The accelerator grid, visible at the top of the thruster, is attached 10 and electrically isolated from a stainless steel mounting ring with ceramic standoffs. The screen grid located directly below the accelerator grid is attached physically and electrically to the mounting ring with stainless steel spacers. The discharge chamber and oven arc sandwiched between the. optics system and a retaining plate at the upstream end of the thruster. Two of the four rods used to attach the mounting ring to the plate arc clearly visible in Fig. 2. Also visible in Fig. 2, arc the anode heater wires and the. oven diameter heater wire. The boron-nitride ring used 10 electrically isolate the anode from the oven can aiso be seen in [he, photograph.

Subsequent [0 obtaining these photographs, the oven and anode were wrapped with tantalum foil to provide thermal radiation shielding. When the engine is mounted in the vacuum chamber the retaining plate is mounted on ceramic standoffs so that the. engine can be biased to the desired potential. To shield the thruster from ambient plasma a ground screen surrounds the entire engine except for the optics system. In addition, an electromagnet capable of producing magnetic fields as high as 0.02 Tesla is placed around the thruster.

The ion optics system was removed to provide a vie. w of the interior of the discharge chamber in Fig. 3. Visible is the baffle plate used to provide fullerene flow between the. oven and discharge chamber. The twin bore. ceramic tube used to isolate the filament cathode leads from the anode earl also be seen. Also note the small lube, located at the center of the oven, which is used to direct fullerenes toward the QCM.

Beam Diagnostics

To determine the species of ions being extracted from the ion engine an ExB probe designed 10 provide 24 a.m.u. resolution at 720 a.m.u. was designed and constructed. A schematic of [he. probe is shown in Fig. 4. The probe operates hy collimating a small fraction of the approaching beam ions with the 0.?5 mm by 19 mm slits at each end of the 2.5 cm square., 2.'/.3 cm long collimator tube. The downstream end 0(the collimator tube extends 2.5 cm into the ExB section to minimize fringe field effects. Ions entering the 61 cm long ExB section encounter a permanent-magnet induced, 0.15 Tesla B field and an E-field which can be varied by changing the potential difference between the plates which are spaced 3.5 cm apart. The E-field plates are made from channels which arc 3.6 cm long in the direction parallel to the collimator slits and have legs that arc 1.1 cm long perpendicular to the slits. At a given plate potential difference all ions, except those in a narrow velocity range, arc deflected away from the collector. The collector is housed in a 7.0 cm long steel tube equipped with a 0.25 mm by 19 mm entrance slit; this tube also extends 2.5 cm into the ExB region. Because [he. probe distinguishes based on ion velocity, ions with different masses but the same kinetic energy arc sensed at different plate potential di fferences. By sweeping the plate potential difference, plots of current reaching the collector as a function of this difference can be generated; various species of ions can be identified from such plots.

Preliminary calibration of the ExB probe was done using a mixture of xenon. krypton and argon. Shown in Fig. 4 is an ExB probe trace obtained with a 1,5 keV ion beam extracted from the engine operating with a 58 V, 0.95 A discharge. Although the engine could be operated on the gas mixture at discharge voltages as low at 25 V, the high discharge voltage was used to insure, that detectable levels of doubly ionized gas atoms would appear in the traces. Identified on the trace arc singly ionized xenon at 213 V, krypton at 267 V and argon at 391 V. The doubly ionized xenon peak appears at 303 V while the doubly ionized krypton peak overlaps the argon peak at 381 V. The triple xenon peak should appear at 372 V and is overlapped by the doubly ionized krypton peak. The triply ionized krypton peak appears at 469 V. Using this calibration singly and doubly ionized C_{60} should appear at 91 V and 129 V, respectively. The fullerene used for the.sc experiments had a small amount (less than 5%) of C_{70} in the powder which was vaporized. The singly and doubly ionized C_{70} should appear at 84 V and 119 **V**, respectivel y.

The ExB probe is capable of resolving isotopes of [he. calibration gases. The main isotopes of xenon arc Xe_{136} (().()89), Xe_{134} ([).]04), Xe_{132} **(0.2.69)**, Xe_{131} **(0.212)**, Xe_{130} (0.041), Xe_{129} (0.264), and Xe_{128} (0.019). The main isotopes of krypton arc Kr_{86} (0.173), Kr_{84} (0.570), Kr_{83} (0.1 15), Kr_{82} (0.1 16), and Kr_{80} (0.0225). Argon has one main isotope, Ar_{40} (().9995). Here [he. subscript after the gas symbol denotes the atomic mass of the isotope and the number in brackets is the mole fraction of each isotope. The peaks due. to singly ionized xenon and krypton arc enlarged in Fig. 5. Four isotopes of xenon (Xe_{136}, Xe_{134}, Xe_{132}, Xe_{129}) can be resolved. The Xe_{131} peak overlaps the Xc132 peak arid is cannot be resolved in this plot. The other xenon isotopes have a small mole fraction compared to the five isotopes listed and also are not resolved in Fig. 5. The four major krypton isotopes (Kr_{86}, Kr_{84}, Kr_{83}, Kr_{82}) arc resolved in Fig. 5. Probe mass resolution is given by

$$M/AM \ . \ [2q/(MAV)]^{1/2} A \qquad \text{(Eq. 5)}$$

where M is the mass of the. particle, q is the. charge of the particle, AV is the potential through which the particle has been accelerated and A is a constant associated with the probe geometry and magnetic field strength. Since the probe can resolve 1 a.m. u. at 84 a.m.u. the probe should be capable of resolving 25 a.m.u. at 720 a.m.u. This is good enough to resolve C_{60} and C_{58} as well as smaller fullerenes.

Composition of Extracted Fullerene Ion Beam

The Ex B probe was used to determine the spc.tics of ions being extracted from the. ion engine. Ideally only singly and doubly ionized C_{60} would appear without any fragment ions. However, it can be seen from the trace in Fig. 6 that [his is not the case. Shown is an ExB trace obtained with the ion engine operating on fullerenes with a 39 V, 0.74 A discharge. The fullerene flow rate varied between 0.17 and O.18 mg/s while the trace was being taken. The flow rate was at its maximum valuer when the plain potential difference was about 130 V and was at the minimum value when the [race started at 60 V and ended at 2(K) V. The net-accelerating voltage was 1.5 kV while the total accelerating voltage was 2.0 kV. The beam current varied between 7.5 and 8.5 mA while. the trace was being obtained; the variation correlated with the variation in fullerene mass flow rate.

As seen in the trace singly ionized fullerene fragment ion from C_{60-2n} (n=0, 1,...,13) arc. evident. A significant signal duc to doubly ionized fullerene fragment ions is also seen in Fig. 6. It is evident that the magnitude of the signal decreases for fragments smaller than C_{50}; however, the peak at the location of doubly ionized C_{40} is larger [ban that for C_{42}^{+}. This occurs because C_{60}^{+++} appears at the same plate potential difference as C_{40}^{++} At plate. potential differences greater than that for C_{40}^{++} (1 S7.5 V), double and triple ion peaks overlap and it bc.comes difficult to resolve some of the peaks.

It is desirable to determine the fraction of fullerene fragments ions which are extracted from the ion engine. Ideally if peaks duc to different species of ions do not overlap in the ExB probe traces, the current density al the probe collimator entrance slit is proportional to the peak height for that species. However, in the trace shown in Fig. 6, the peaks do overlap and therefore the peak heights do no[indicate the true current density. The actual current density can be bracketed by taking the peak heights from the trace ([his provides an overestimate) and by using the distance that the. peak rises above the valleys on either side (this provides an underestimate). When this is done for the data in Fig. 6, the upper and lower bound on fragment current fraction for singly ionized fullerenes is 0.689

and 0.804. Peaks for C_{60}^{+} through C_{32}^{+} were included in the calculation. For doubly ionized fragment current peaks from C_{60}^{++} to C_{42}^{++} are included in the computation. Peaks below C_{42}^{++} were not included because triple ions are mixed in with the doubles peak. The fragmentation current fraction for double ions is bounded between 0.811 and 0.8547. From these data it is evident that a large fraction of the fullerenes in the discharge chamber dissociate before they are extracted. It is noted that these data were obtained with the thruster operating at temperatures below 910 K where thermal decomposition of fullerenes is negligible. Thus it is apparent that the observed fullerene degradation is due to processes inherent to producing a plasma.

Further evidence to support this claim is found from examination of the ion engine after a typical experiment. After experiments the ion engine is disassembled and examined. When the oven is examined no evidence of fullerene fragmentation is observed. However, when the discharge chamber interior is examined, a black residue coats the entire inside of the chamber. This residue is collected and weighed and typically it accounts for 1/3 to 2/3 of the fullerene mass which was placed in the oven at the start of the experiment. Chemical analysis of this residue shows that it does not contain fullerenes.

These results seem to be at odds with the cross-section experiments discussed in the introduction where 45 eV electrons were required before fragment ions were detected. This discrepancy can be resolved if it is noted that elect Ion impact ionization produces metastable C_{60}^{+} ions which have a half-life before they fragment. In the cross-section experiments fullerenes are accelerated toward the mass spectrometer within 1 10 10 μs of the time at which they are produced. Typical residence times for fullerenes in an ion engine are on the order of 1 ms which is two to three orders of magnitude longer. Because of the difference in time scales the probability that a fullerene will dissociate before it is accelerated is much higher in an ion thruster even with lower energy electrons. Although only positive ion fragmentation has been discussed here, there are many more process occurring in the discharge chamber which can pump energy into fullerenes. These include negative ion formation, and ions impacting the discharge chamber walls with kinetic energies on the order of the discharge voltage. Each of these processes can impart internal energy to fullerenes and lead to their eventual fragmentation.

Conclusions

Experiments were conducted which show substantial fullerene fragmentation occurs in ion engines operating at temperatures below 910 K. The dissociation was found to be caused by processes inherent to producing a plasma in a discharge chamber. Because fullerene fragmentation in a thruster reduces the thruster efficiency and if severe enough can result in shorting of electrical components, a method of eliminating fragmentation before the acceleration must be found in order for fullerenes to be a useful propellant. Two possibilities exist for accomplishing this. One is to ionize fullerenes without pumping large amounts of energy into internal energy which subsequently causes dissociation. Surface or field ionization might be used to accomplish this. The second possibility is suggested by the low fragmentation rate observed on the short time scales used in the cross-section experiments. Namely, fullerenes must be processed on a much shorter time scale than those typical of ion thrusters to avoid fragmentation before they are accelerated. To accomplish this micro-thrusters with dimensions on the order of 0.1mm would be required.

Acknowledgments

The research described in this paper was conducted at the Jet Propulsion Laboratory, California Institute of Technology, under contract with the National Aeronautics and Space Administration.

The authors thank A. G. Owens, W. R. Thogmartin and R. L. Toomath for their technical assistance.

References

1. Leifer S., Rapp D., Saunders W., "Electrostatic Propulsion Using C_{60} Molecules," AIAA Journal of Propulsion and Power, Vol. 8(6), 1993, p.1297

2. Torres E., Matossian J., Williams J., Martinez-Sanchez M. "Predictions of the Performance of an Ion thruster Using Buckminsterfullerene as the Propellant," AIAA/SAE/ASME/ASEE 29th Joint Propulsion Conference AIAA 93-2494, Monterey, (California, 1993.

3. Anderson J., Fitzgerald D., "Experimental Investigation of Fullerene Propellant for Ion Propulsion," IEPC-93-033, Seattle, Washington, Sept. 1993.

4. Hruby V., Martinez-Sanchez M., Bates S., Lorents D., "A High Thrust Density, C_{60} Cluster Ion Thruster," 25th AIAA Plasmadynamics and Lasers Conference AIAA 94-2466, Colorado Springs, Colorado, June 1994.

5. Nakayama Y., Takegahara H., "Fundamental Experiments of C_{60} Applic.alien 10 Ion Thruster", **2.4** th International Electric Propulsion Conference IEPC-95-88, Moscow, Russia, Sept. 1995.

6. Horak P., Gibson **U.**, "Broad Fullerene-Ion Beam Generation and Bombardment Effects," Applied Physics Letters, 65(8), **1994**, p.968.

7. Fang D., Gao 11., Lu F., Tang J., Yang F., "Production of C_{60}/C_{70} Ion Beams," Chinese Physics Letters, Vol. 10(8), 1993, p. 453.

8. Brophy J., Polk J., Pless 1.., "Test-to-Failure of a Two-Grid, 30-cm-dia. Ion Accelerator System," IEPC-93-1 72, 23rd International Electric Propulsion Conference, Seattle, Washington, Sept. 1993.

9. Kratschmer W., Lamb L., Fostiropoulos K., Huffman D., "Solid C_{60}-a New Form of Carbon," Nature, Vol. **347, 1990,** p.354.

10. Foltin M., Lezius M., Scheier P., and Mark "1". D., "On the Unimolecular Fragmentation of C_{60}^+ Fullerene ions: The Comparison of Measured and Calculated Breakdown Patterns," J. Chem. Phys., Vol. .98(12), 1993, pp. 9624-9634.

11. Worgotter R., Dunser B., Scheier P. ,Mark"l". D., Foltin M., Klots C. E., Laskin J., and Lifshitz C., " Self-Consistent Determination of Fullerene Binding Energies BE $(C_n^+-C_2)$, n= 58,...,44," J. Chem. Phys., Vol. 104(4), 1996, pp. 1??s-1?31.

12. Kolodney E., Tsipinyuk B., and Budrevich A., "The Thermal Energy Dependence (10-20 eV) of Electron Impact Induced Fragmentation of C_{60} in Molecular Beams: Experimental arid **Model** Calculations," J. Chem . Phys., Vol. 102(23), 1995, pp. 9263-9275.

13. O'Brien **S.**, Heath J., Curl R., Smalley R., "Photophysics of Buckminsterfullerene and Other Carbon Cluster Ions," Journal of Chemical Physics, Vol. 88, 1988, p. 220.

14. Busmann 11., Lill "1'., et al, "Collision Induced Fragmentation and resilience of scattered C_{60}^+ Fullerenes," Surface Science , Vol. 272, 1992, pp. 146-153.

15. Whetten R. , Yeretzian C., St John P., "Cleavage Patterns of Carbon Clusters from Impact-Induced Fragmentation Of C_N^-, N=10 SO," International Journal of **Mass** Spectrometry and Ion Processes, Vol. 138, 1994, pp. 63-76.

)6. Yoo R., Rustic B., Berkowitz 1., "Vacuum Ultraviolet Photoionization Mass Spectrometric Study of C_{60}," Journal of Chemical Physics, Vol. 96(2), 1992, pp. 91 1-918.

17. Von Gersum S., Kruse T., Roth P., "Spectral Emission During High Temperature Pyrolysis of Fullerene C_{60} in Shock Wave.s, " Berichte Bunsen-Gesellschaft fur Physikialische Chemie, Vol. 98(7), 1994, p. 979.

18. Kolodney E., Tsipinyuk B., Budrevich A., "The Thermal Stability and Fragmentation of C_{60} Molecules up to 2000 K on the Millisecond l"ilnc.scale, " Journal of Chemical Physics, Vol. 100(11), 1994, p. **8452.**

19. Sundar C., Bharathi **A.,** Harihan Y., Janaki J., Sankare Sastry V., Radhakrishnan T., "Thermal Decomposition of C_{60}," Solid State Communications, Vol. 8A(8), 1992, p. **823.**

20. Frum C., Engleman R., Hedderich H., Bernath P., Iamb 1.., Huffman D., "The Infrared-Emission Spectrum of Gas-Phase C_{60} (Buckminsterf ullerene), " Chemical Physics Letters, **vol.** 176(6), 1991, p. 504.

21. Leifer S., Goodwin D., Anderson M., Anderson J., "Thermal Decomposition of a Fullerene Mix," Physical Review B, Vol. 51(1 S), 1995, p. 9973.

22. Abrefah J., Balooch M., Sickhaus W., (lander D., "Vapor Pressure of Buckminsterfullerene," Applied Physics Letters, Vol. 60(1 l), 1992, p. 1313.

23. Tokmakoff A., Haynes D., George S., "Desorption Kirlc.[its of C_{60} Multilayers from $Al_2O_3(0001)$," Chemical Physics Letters, Vol. 186(4,5), 1991, p. 450.

24. Mathews C., Sai Baba M., Lakshmi Narasimhan 'i'., Balasubramanian R. Sivaraman N,, Srinivasan 'T'., Vasudeva Rao }'., "Vaporization Studies on Buckminsterfu llerene," Journal of Physical Chemistry, Vol. 96, 1992, p. 3566.

25. Pan (''., Chandrasekharaiah M., Agan D., Hauge R., Margrave J., "Determination of Sublimation Pressures of C_{60}/C_{70} Solid Solution," Journal of Physical Chemistry, **Vol.** 96(16), 1997, p. 6752..

?.6. Takegahara 11., Naka yama Y., "C_{60} Molecule as a Propellant for Electric l'repulsion," 23rd International Electric Propulsion Conference IEPC-93-032, Seattle, Washington, Sept. 1993.

27 Anderson J., Fitzgerald D., Leifer S., Mueller J., "Design arid Testing of a Fullerene RF Ion Engine" AIAA 95-2664, San Diego, California, July 1995.

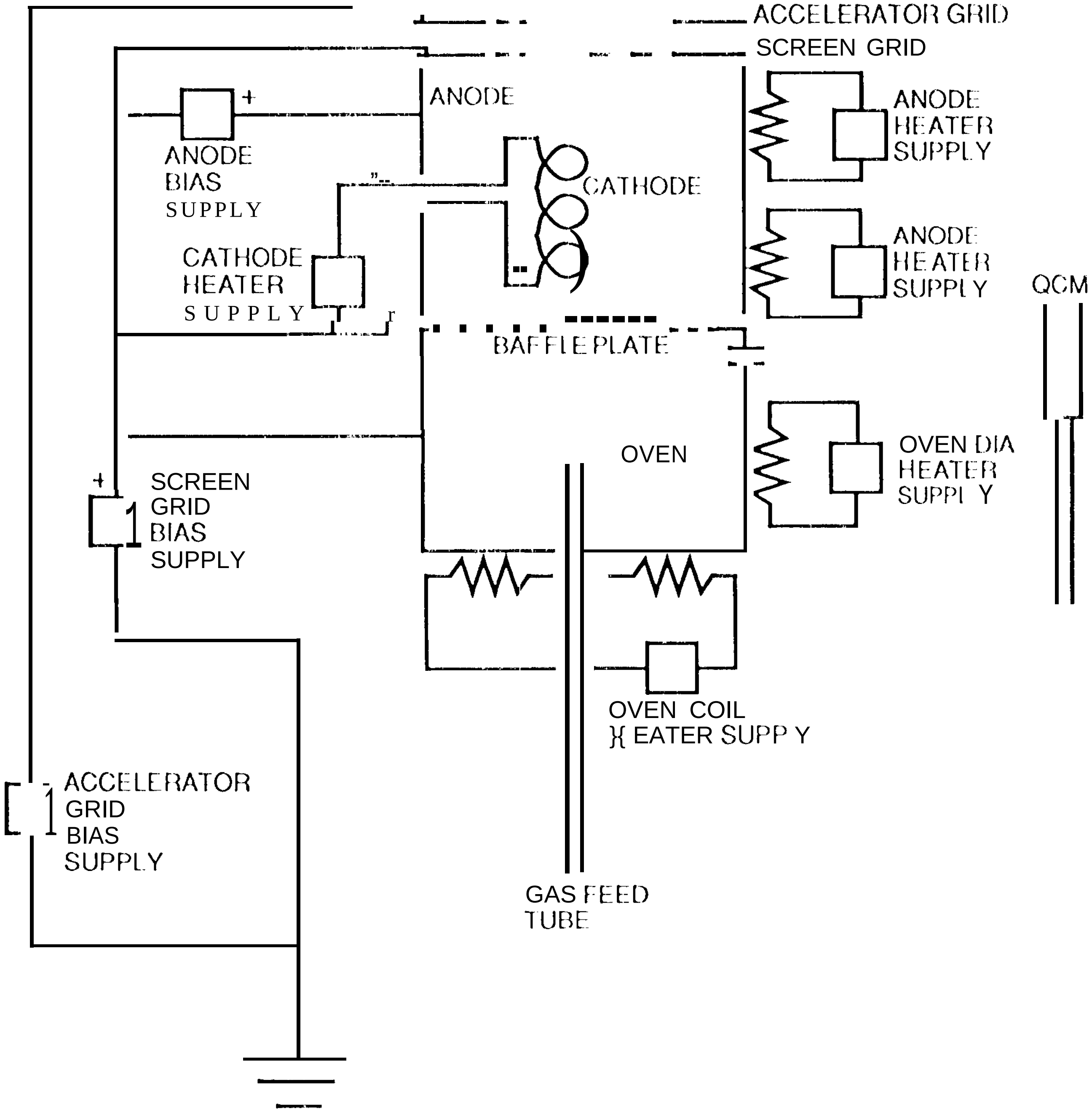
ACCELERATOR GRID
SCREEN GRID
ANODE
ANODE BIAS SUPPLY
CATHODE
ANODE HEATER SUPPLY
ANODE HEATER SUPPLY
CATHODE HEATER SUPPLY
QCM
BAFFLE PLATE
OVEN
OVEN DIA HEATER SUPPLY
SCREEN GRID BIAS SUPPLY
OVEN COIL HEATER SUPPLY
ACCELERATOR GRID BIAS SUPPLY
GAS FEED TUBE

Fig. 1.

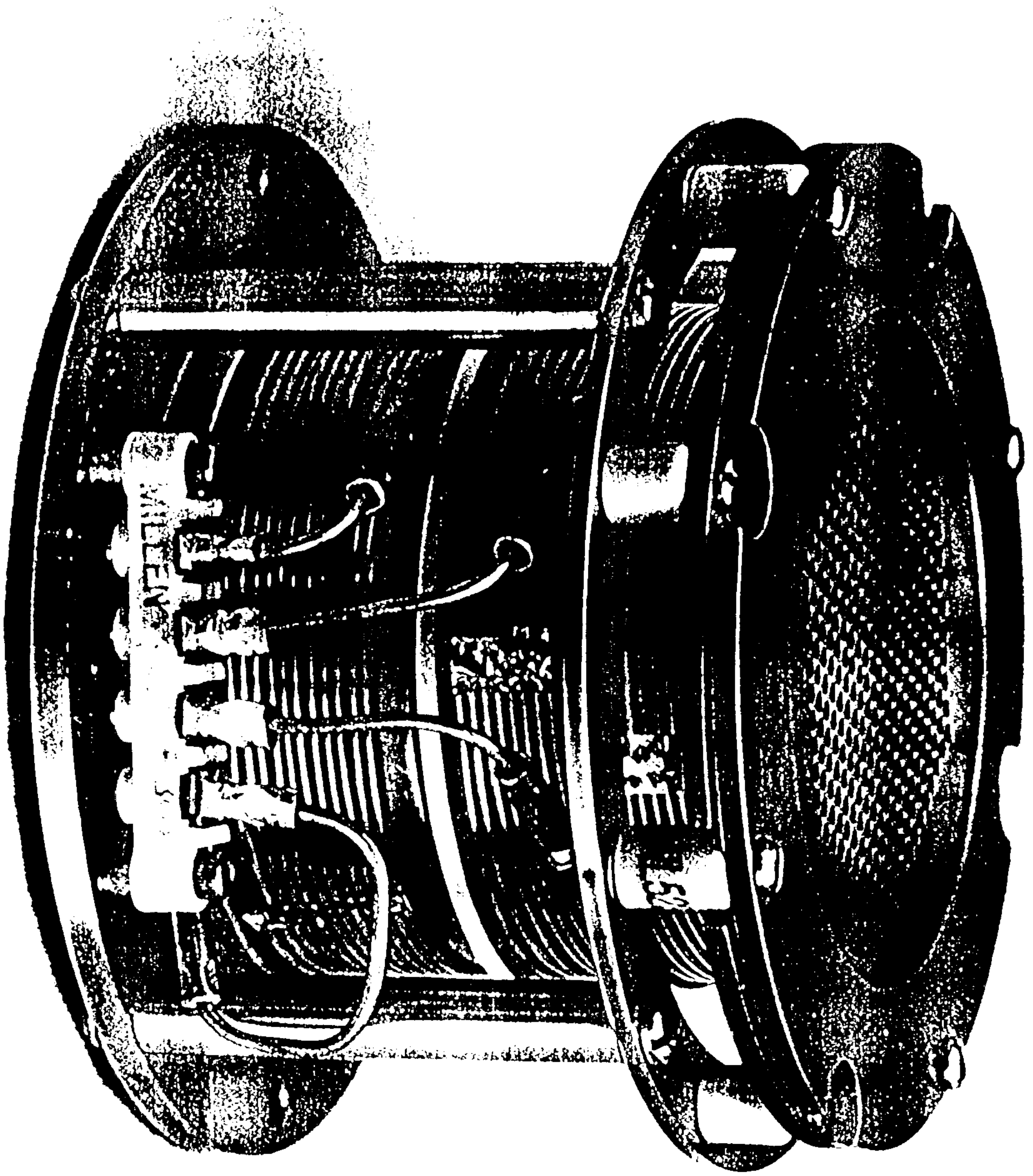
MILLEN

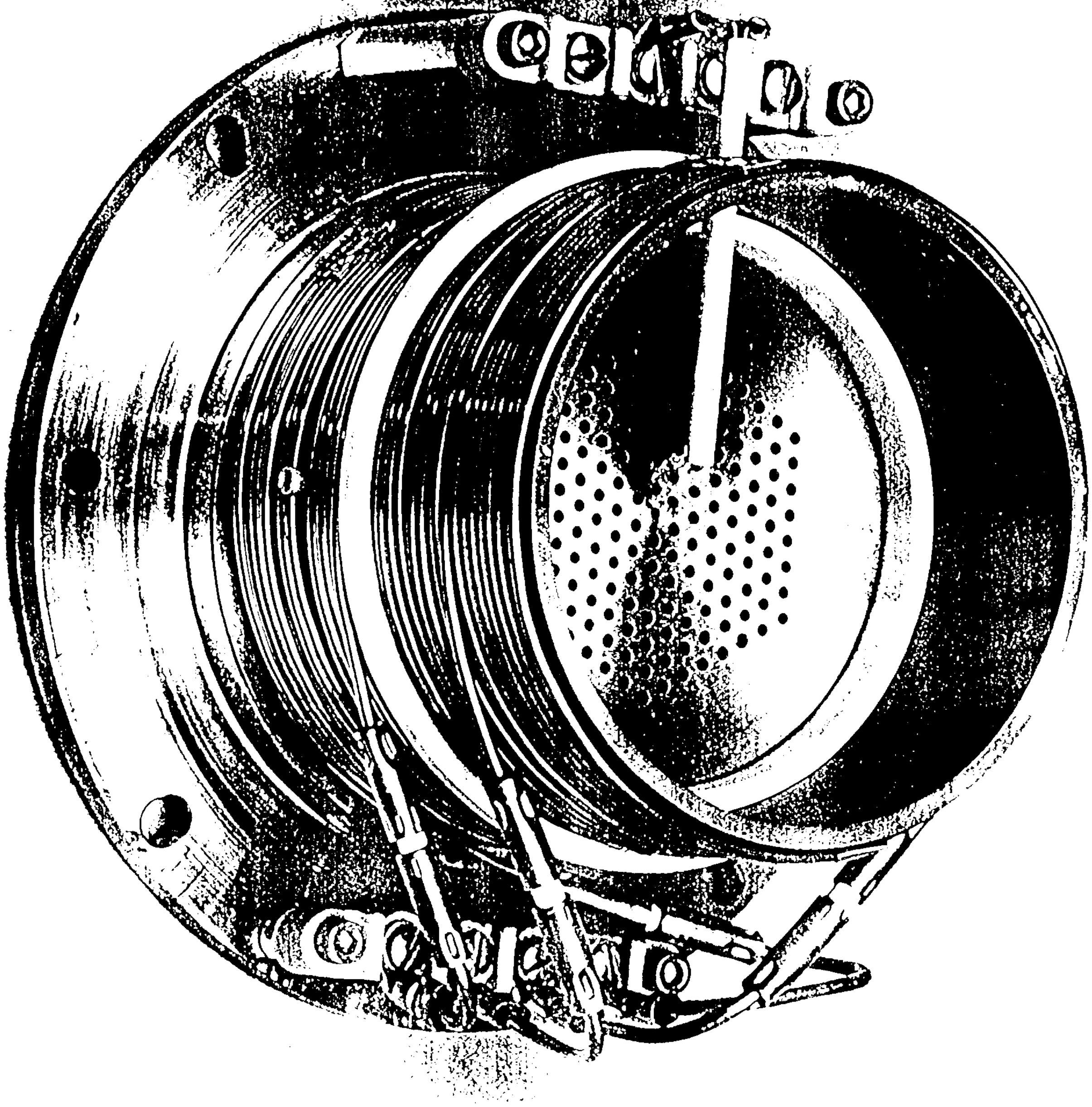

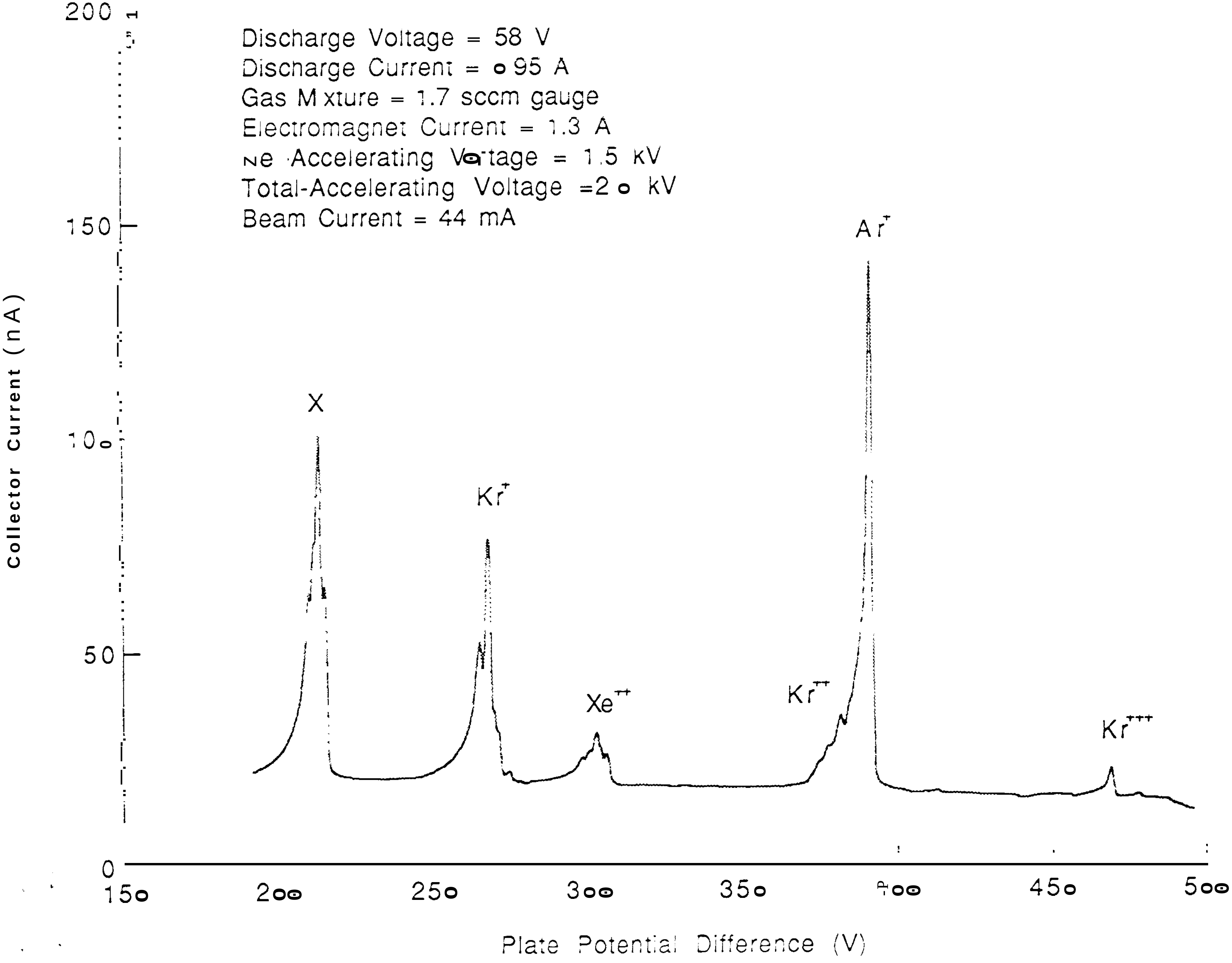

Discharge Voltage = 58 V
Discharge Current = o 95 A
Gas M xture = 1.7 sccm gauge
Electromagnet Current = 1.3 A
Xe Accelerating Voltage = 1.5 kV
Total-Accelerating Voltage =2 o kV
Beam Current = 44 mA
X
Kr+
Xe++
Kr++
Ar+
Kr+++
Collector Current (nA)
Plate Potential Difference (V)
0
50
100
150
200
150
200
250
300
350
400
450
500

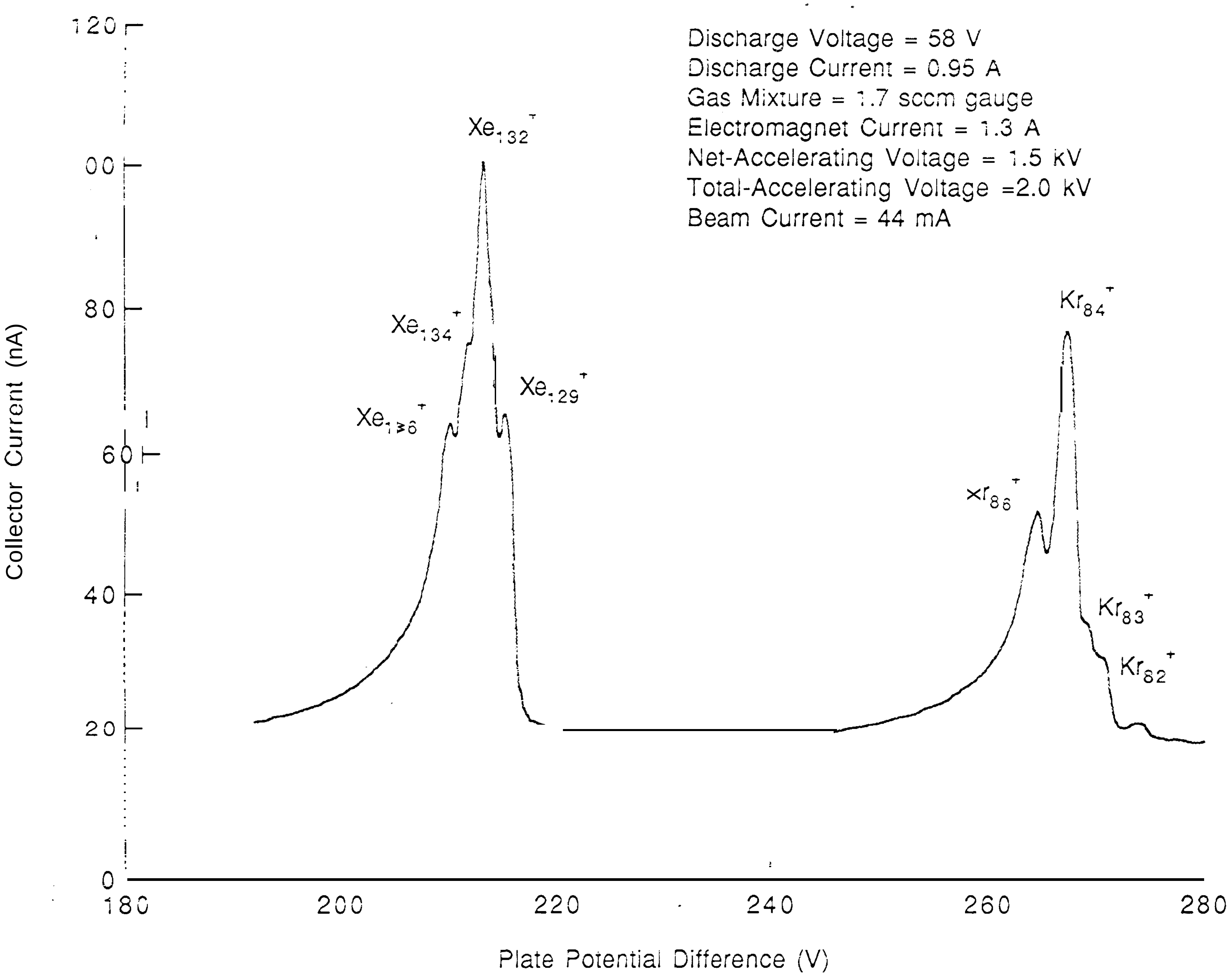
Collector Current (nA)
Plate Potential Difference (V)
Discharge Voltage = 58 V
Discharge Current = 0.95 A
Gas Mixture = 1.7 sccm gauge
Electromagnet Current = 1.3 A
Net-Accelerating Voltage = 1.5 kV
Total-Accelerating Voltage =2.0 kV
Beam Current = 44 mA
Xe_{132}^+
Xe_{134}^+
Xe_{136}^+
Xe_{129}^+
Kr_{84}^+
Kr_{86}^+
Kr_{83}^+
Kr_{82}^+

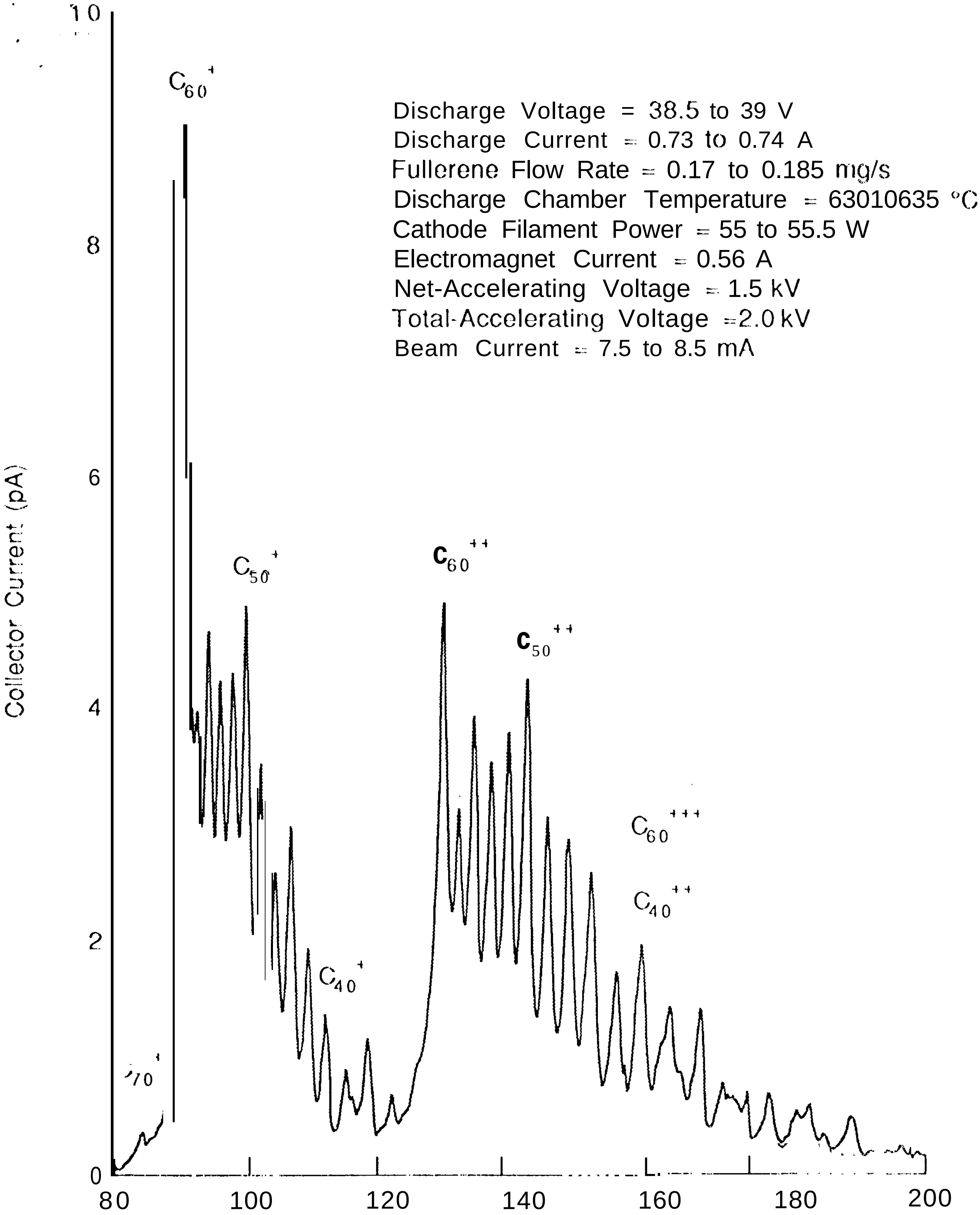

Discharge Voltage = 38.5 to 39 V
Discharge Current = 0.73 to 0.74 A
Fullerene Flow Rate = 0.17 to 0.185 mg/s
Discharge Chamber Temperature = 63010635 °C
Cathode Filament Power = 55 to 55.5 W
Electromagnet Current = 0.56 A
Net-Accelerating Voltage = 1.5 kV
Total-Accelerating Voltage = 2.0 kV
Beam Current = 7.5 to 8.5 mA
C_{60}^{+}
C_{50}^{+}
C_{40}^{+}
C_{60}^{++}
C_{50}^{++}
C_{60}^{+++}
C_{40}^{++}
Collector Current (pA)
Plate Potential Difference (V)
0
2
4
6
8
10
80
100
120
140
160
180
200

Fig 6